

Design of a Novel Two Degree-of-Freedom Ankle-Foot Orthosis

Abhishek Agrawal

Graduate Student

Mechanical Engineering Department
University of Delaware
Newark, Delaware 19716
Email: agrawala@me.udel.edu

Sai K. Banala

Graduate Student

Mechanical Engineering Department
University of Delaware
Newark, Delaware 19716
Email: sai@udel.edu

Vivek Sangwan

Graduate Student

Mechanical Engineering Department
University of Delaware
Newark, Delaware 19716
Email: sangwan@udel.edu

Sunil K. Agrawal

Professor

Mechanical Engineering Department
University of Delaware
Newark, Delaware 19716
Email: agrawal@udel.edu

Stuart A. Binder-Macleod

Professor and Chair

Department of Physical Therapy
University of Delaware
Newark, Delaware 19716
Email: sbinder@udel.edu

An ankle-foot orthosis (AFO) is commonly used to help subjects with weakness of ankle dorsiflexor muscles due to peripheral or central nervous system disorders. Both these disorders are due to the weakness of the tibialis anterior muscle which results in lack of dorsiflexion assist moment. The deformity and muscle weakness of one joint in the lower extremity influences the stability of the adjacent joints, thereby requiring compensatory adaptations. We present an innovative ankle-foot orthosis (AFO). The prototype AFO would introduce greater functionality over currently marketed devices by means of its pronation-supination degree-of-freedom in addition to flexion/extension. This orthosis can be used to measure joint forces and moments applied by the human at both joints. In future, by incorporation of actuators in the device, it will be used as a training device to restore a normal walking pattern.

1 Introduction

During the swing phase of gait cycle, the ankle is dorsiflexed (rotated upward) to allow the foot to clear the ground while the extremity is advanced. Hyperactive plantarflexor (muscle rotating foot downward) or weak dorsiflexor muscle may result in insufficient dorsiflexion, which must be compensated for by alterations in the gait patterns so that the

toes do not drag. This insufficient dorsiflexion during the swing phase of gait is termed as foot-drop. In addition to the toes dragging, the foot may become abnormally supinated at the end of the swing phase of gait cycle, which may result in an ankle sprain or fracture when weight is applied to the limb. Foot-drop is commonly seen in subjects who have had a stroke or who have sustained a peroneal nerve injury. The details of the foot kinematics are provided in the next section.

There are several possible treatments for foot-drop that use pharmacological, surgical, or orthotic interventions. Of these, orthotic treatment is the most common. Orthotic devices are intended to support the ankle, correct deformities, and prevent further injuries. A key goal of orthotic treatment is to assist the patient in achieving a measure of normal function. Ferris et. al. [1] proposed an ankle-foot orthosis powered by artificial muscles. The orthosis has two pneumatic muscles to control the dorsiflexion and plantarflexion motion of the ankle. Yamamoto et. al. [2] developed a dorsiflexion assist orthosis controlled by a spring. Dorsiflexion correction is achieved via the compression force of a spring within the assistive device. When the ankle joint rotates into plantarflexion, a piston compresses the spring and an assist moment proportional to the plantarflexion angle is generated. Blaya [3] proposed an active ankle-foot orthosis with one

degree-of-freedom. The active ankle-foot orthosis comprises a force-controllable series elastic actuator (SEA) capable of controlling orthotic joint stiffness and damping for plantar and dorsiflexion ankle motions. Other works have focused on improving the comfort and techniques for weight reduction of an ankle-foot orthosis using finite element modeling and experimental testing [4, 5]. A perspective on biomedical assist devices is provided in [6]. There are a number of commercially available ankle-foot orthoses. All of these orthoses are single axis or are elastically deformable. The pronation-supination motion in these orthoses are accommodated through the flexibility of the polymeric material. The limitation in normal ankle pronation-supination adds to the discomfort and does not provide a natural motion to the ankle.

In this paper, an ankle-foot orthosis with two degrees-of-freedom is proposed. The two degree-of-freedom orthosis assumes that the foot is connected to the shank by a serial chain with two degrees-of-freedom. The first angle degree-of-freedom in the chain is dorsiflexion-plantarflexion while the second is pronation-supination. Both joints are fitted with encoders. The device also has two force-torque sensors in its design. Using the data from force-torque sensors and encoders, the torques applied by the human at each joint can be computed. The device can be used as a stand alone measurement device to measure forces and torques at the joints during isometric or non-isometric contractions and throughout the range of motion of the ankle. This paper describes this device, its kinematic model, the design of the device, Newton-Euler analysis to determine the human joint forces and torques, analysis of experimental data, and possible applications of this device for rehabilitation.

2 Kinematic Model

The overall motion of the ankle is complex [7, 8]. In this paper we are concentrating on two degrees-of-freedom. The first degree-of-freedom is a rotation in the vertical plane about an axis passing through the ankle joint. This axis is shown as Z_1 in Fig. 1 and this motion is known as dorsiflexion-plantarflexion (D/P) motion. The second degree-of-freedom is a rotation about an axis shown as Z_2 in Fig. 1. This motion is known as pronation-supination (P/S) motion. In this paper, the lower leg (shank and foot) is considered to be composed of three rigid links connected by two revolute joints. The first rigid link is the shank segment. The second rigid link represents the rear foot comprising of the talus bone, which is the bone between the D/P axis and the P/S axis. The third rigid link represents the front foot comprising of the bones after the P/S axis [8]. The front foot comprises of a large number of small bones. It has a complicated flexible motion that is hard to model [8–10]. In this paper, we are concentrating on the motion of the rear foot and for the purpose of modeling both segments of the foot are assumed to be rigid links, and the dorsiflexion-plantarflexion and pronation-supination motions are approximated by revolute joints.

The orientations of the two joint axes considered in this

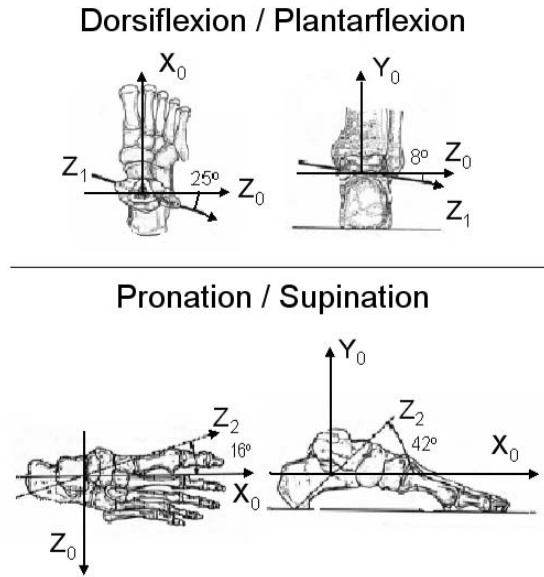


Fig. 1. Orientations of dorsiflexion-plantarflexion joint axis (\vec{Z}_1) and pronation-supination joint axis (\vec{Z}_2) and their projection angles [7, 8].

study are shown in Fig. 1. It shows the projection of the joint axes in the frame attached to the shank ($\vec{X}_0, \vec{Y}_0, \vec{Z}_0$) [7, 8]. The axis \vec{Z}_0 represents the knee joint axis. This projection is taken when the foot is resting firmly on the ground and the shank is perpendicular to the ground.

The Denavit-Hartenberg (DH) parameters of the kinematic model from the information shown in Fig. 1 were determined. Average lengths of the links were obtained from anthropomorphic data [13]. We determined the unit vectors \vec{Z}_1 and \vec{Z}_2 in the frame \vec{Z}_0 using the relation between spherical and Cartesian coordinates shown below.

$$x = r \cos \gamma \sin \phi, \quad (1)$$

$$y = r \sin \gamma \sin \phi, \quad (2)$$

$$z = r \cos \phi. \quad (3)$$

Because the projections of \vec{Z}_1 and \vec{Z}_2 in \vec{Z}_0 are known, we can compute their spherical coordinates: $\gamma_1 = 196.7^\circ$, $\phi_1 = 25.9^\circ$ for \vec{Z}_1 and $\gamma_2 = 42^\circ$, $\phi_2 = 102.0^\circ$ for \vec{Z}_2 .

Next, we defined \vec{X}_1, \vec{Y}_1 axes and \vec{X}_2, \vec{Y}_2 axes as follows:

$$\vec{X}_{i+1} = \frac{\vec{Z}_i \times \vec{Z}_{i+1}}{\|\vec{Z}_i \times \vec{Z}_{i+1}\|} \quad (4)$$

$$\vec{Y}_{i+1} = \frac{\vec{Z}_{i+1} \times \vec{X}_{i+1}}{\|\vec{Z}_{i+1} \times \vec{X}_{i+1}\|} \quad (5)$$

The Denavit-Hartenberg parameters θ_i, α_i, a_i and d_i were used to locate the frames on the bodies. Once all the unit vectors \vec{X}_i, \vec{Y}_i and \vec{Z}_i are known, θ_i and α_i can be computed

using vector algebra. a_i and d_i were computed using anthropomorphic data and loop closure equation,

$$T_0^3 = T_0^1 T_1^2 T_2^3, \quad (6)$$

where T_i^{i+1} denotes the transformation matrix between two successive bodies i and $i + 1$. In the nominal configuration of the foot, when the foot is flat on the ground and perpendicular to the shank, the DH parameters computed are given below:

$$T_0^1, \theta_0 = 286.7^\circ \text{ and } \alpha_0 = 25.9^\circ$$

$$T_1^2, \theta_1 = 210.6^\circ \text{ and } \alpha_1 = 125.0^\circ$$

$$T_2^3, \theta_2 = 13.1^\circ \text{ and } \alpha_2 = 0^\circ$$

θ_i are the joint variables, which take the particular values shown above for the mentioned configuration of the foot.

Once all these parameters are calculated, the complete kinematic model is known.

3 Design of The Orthosis

An engineering prototype of the two degrees-of-freedom (dof) ankle-foot orthosis (AFO) was fabricated at the University of Delaware. The orthosis is composed of three links connected by two revolute joints corresponding to the three segments and two degrees-of-freedom of the foot described in the previous section. These three links are shown in Fig. 2. The machine shank gets rigidly attached to the human shank by means of a brace and Velcro straps. The third link of the orthosis gets rigidly attached to the third i.e. the terminal segment of the foot by means of a brace and Velcro straps. The second link of the orthosis is not directly in contact with the second foot segment, i.e., the segment between the P/S and D/P axes but has little relative motion with respect to the segment of the human foot.

Following are the salient features of the orthosis: (i) machine parts are made out of lightweight aluminum. Ball bearings are used at the dorsiflexion-plantarflexion and the pronation-supination joints; (ii) it has braces and Velcro straps to provide a comfortable fit to the user; (iii) limbs are made to be telescopic to accommodate variability in the foot dimensions across human subjects; (iv) Both of the joint axes, Dorsiflexion-plantarflexion axis and Pronation-Supination joint axis are physically located and oriented in the device as described in the kinematic model. The obliquely cut parts labeled “A” and “B” shown in Fig. 3 are used to orient the joint axes. Hence the orientation of the joint axes are fixed. However, the location of the joint axes can be changed to fit the subject, by adjusting the telescopic links in the device. (iv) Both of the joints are fitted with optical encoders to measure the joint angles. (v) Two force-torque sensors are placed on the device. One beneath the “sole” of the device and the other between the human shank and the device shank.

The net weight of the device is 3.7 Kg. By using the force and moment balance equations for the foot and the shank and data from the force-torque sensors and encoders, forces and torques applied by the human at the joints can be calculated. The engineering prototype will be used as a measuring device in experiments with subjects.

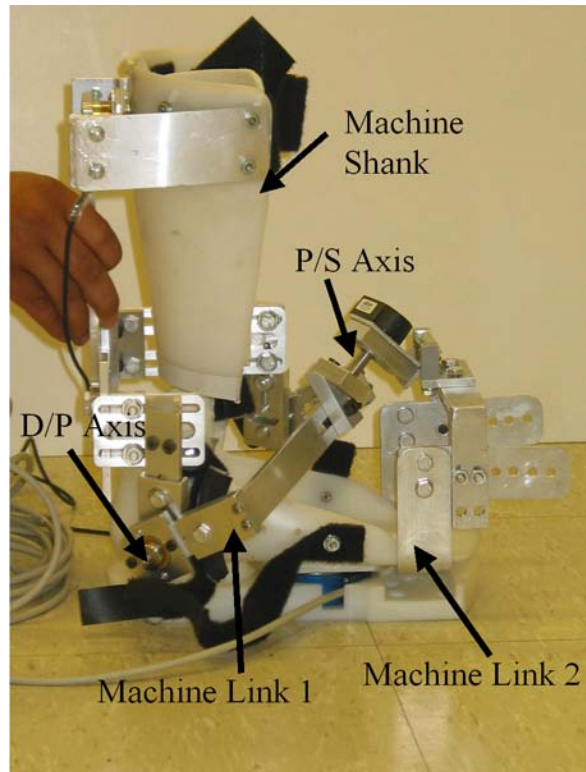


Fig. 2. Assembled ankle-foot orthosis with the shank and the foot brace. It comprises of the three links corresponding to the three segments of the human foot.

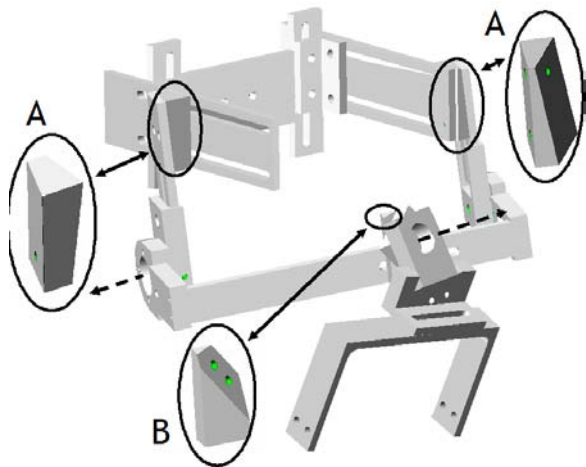


Fig. 3. A 3D AutoCAD drawing of the ankle-foot orthosis fabricated at University of Delaware. Blocks labeled “A” and “B” are used to orient the joint axes.

4 Measuring Joint Forces and Moments

The objective of this device is to measure the forces and torques applied by the human at the D/P and P/S joints. This section describes the Newton-Euler analysis that is used to convert the raw force-torque sensor and encoder data into joint forces and torques. It is mentioned in previous sections that both foot and the device are composed of three links and

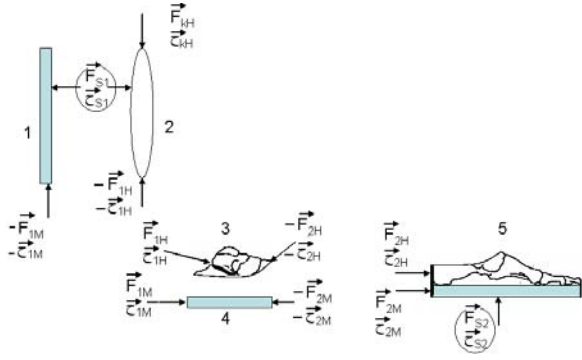


Fig. 4. Free body diagram of human and machine part of the ankle. Oval and bony bodies represent the human segments and the rectangular shaped bodies represent the machine segments. Forces and torques in circles are the sensor forces and torques.

two revolute joints. Using the telescopic joints, the device is adjusted such that the axes of the device coincide with the axes of the human. Then the device is worn by the human as mentioned in the previous section using the straps and braces such that the three human foot and device segments move synchronously with little or no relative motion. The adjustments in the device are varied until the subject is able to execute the normal motion of the foot. It is difficult to get perfect alignment between the human and device axes. Some approaches to get good agreement between them have previously been discussed in [11, 12]. The device and human shanks are kept inertially fixed.

Figure 4 shows the free body diagram of all the bodies in the system. The first and the second bodies in Fig. 4 represent the device and the human shank, which are rigidly attached to each other and are inertially fixed. The third and fourth bodies represent the second segments of the human and device respectively. They are not in direct contact to each other but constrained to move together as a rigid body. The third segment of the device and human are rigidly connected together and they collectively form the fifth body. The forces between these segments are shown in Fig. 4. The subscripts M and H signify the machine and the human components respectively and S implies the sensor component. \vec{F}_{1M} , $\vec{\tau}_{1M}$ and \vec{F}_{2M} , $\vec{\tau}_{2M}$ are the forces and torques between the first-second and second-third links of the device at the D/P and P/S joints respectively. \vec{F}_{1H} , $\vec{\tau}_{1H}$ and \vec{F}_{2H} , $\vec{\tau}_{2H}$ are the forces and torques in between the segments of the human lower leg at the D/P and P/S joints, respectively. The gravitational force is acting at the center of mass of each body and is not shown in the figure for the sake of clarity. \vec{F}_{kH} and $\vec{\tau}_{kH}$ are the force and the torque at the knee joint.

Each of the bodies shown in Fig. 4 has a coordinate frame attached to it. The encoder data along with the geometric details of the device are used to calculate the translational and rotational velocities and accelerations of each of the bodies. Moment balance about the body center of mass and force balance equations are written for each body in its body coordinate frame. All forces and moments are three dimensional. Each body has two vector equations,

i.e., six scalar equations. There are five bodies, so there is a total of thirty equations. The vector unknowns are \vec{F}_{1M} , $\vec{\tau}_{1M}$, \vec{F}_{2M} , $\vec{\tau}_{2M}$, \vec{F}_{1H} , $\vec{\tau}_{1H}$, \vec{F}_{2H} , $\vec{\tau}_{2H}$, \vec{F}_{kH} and $\vec{\tau}_{kH}$ so there are thirty scalar unknowns. The system is uniquely solvable. Solving the force and moment balance equations for the bodies one through five in the order 1-4-5-3-2 gives all the unknown forces and moments without any matrix inversions or iterative procedures. The force due to previous body on the next body is taken as positive and is expressed in the reference frame of the next body. The position vectors and gravity force of a particular body are expressed in the body frame.

Frame 0 is fitted to bodies 1 and 2; bodies 3 and 4 move together, so their coordinate frame have same orientations but different origins. These frames are represented by the same index 1 for the purpose of rotation matrices and finally frame 2 is attached to body 5. Bodies 3 and 4 have the same angular velocity and acceleration, $\vec{\omega}_1$ and $\vec{\alpha}_1$, respectively. Body five has angular velocity and acceleration, $\vec{\omega}_2$ and $\vec{\alpha}_2$, respectively. $\vec{r}_{1M;1}$ represents a vector from the D/P joint to the center of mass of body 1. Other position vectors follow similarly. \vec{F}_w represents the weight vector of respective bodies. Weights of the various human segments are obtained from the average data provided in [13]. The force and moment balance equations for different bodies can be written as follows:

For body 1:

$$-\vec{F}_{S1} + \vec{F}_{w1} - R_0^1 \vec{F}_{1M} = \vec{0}, \quad (7)$$

$$-\vec{\tau}_{S1} - R_0^1 \vec{\tau}_{1M} + \vec{F}_{S1} \times \vec{r}_{S1;1} + (R_0^1 \vec{F}_{1M}) \times \vec{r}_{1M;1} = \vec{0}, \quad (8)$$

For body 4:

$$\vec{F}_{w4} - R_1^2 \vec{F}_{2M} - \vec{F}_{1M} = M_4 \vec{a}_{c4}, \quad (9)$$

$$-R_1^2 \vec{\tau}_{2M} + \vec{\tau}_{1M} - (R_1^2 \vec{F}_{2M}) \times \vec{r}_{2M;4} + \vec{F}_{1M} \times \vec{r}_{1M;4} = I_4 \vec{\alpha}_1 + \vec{\omega}_1 \times I_4 \vec{\omega}_1, \quad (10)$$

For body 5:

$$\vec{F}_{S2} + \vec{F}_{w5} + \vec{F}_{2M} + \vec{F}_{2H} = M_5 \vec{a}_{c5}, \quad (11)$$

$$\vec{\tau}_{S2} + \vec{\tau}_{2M} + \vec{\tau}_{2H} + \vec{F}_{S2} \times \vec{r}_{S2;5} + \vec{F}_{2M;5} \times \vec{r}_{2M;5} + \vec{F}_{2H;5} \times \vec{r}_{2H;5} = I_5 \vec{\alpha}_2 + \vec{\omega}_2 \times I_5 \vec{\omega}_2, \quad (12)$$

For body 3:

$$\vec{F}_{w3} - R_1^2 \vec{F}_{2H} + \vec{F}_{1H} = M_3 \vec{a}_{c3}, \quad (13)$$

$$-R_1^2 \vec{\tau}_{2H} + \vec{\tau}_{1H} - (R_1^2 \vec{F}_{2H}) \times \vec{r}_{2H;3} + \vec{F}_{1H} \times \vec{r}_{1H;3} = I_3 \vec{\alpha}_1 + \vec{\omega}_1 \times I_3 \vec{\omega}_1, \quad (14)$$

For body 2:

$$\vec{F}_{S1} + \vec{F}_{w2} - R_0^1 \vec{F}_{1H} + \vec{F}_{kH} = M_2 \vec{a}_{c2}, \quad (15)$$



Fig. 5. Orientations of the D/P and P/S frame. This picture is representative of only the orientations of the frame and not the locations. The frames are placed at the actual joint in the human foot.

$$\begin{aligned} \vec{\tau}_{S1} - R_0^1 \vec{\tau}_{1H} + \vec{\tau}_{kH} + \vec{F}_{S1} \times \vec{r}_{S1;2} - (R_0^1 \vec{F}_{1H}) \times \vec{r}_{1H;2} \\ + \vec{r}_{kH;2} \times \vec{F}_{kH} = I_2 \ddot{\alpha}_0 + \dot{\omega}_0 \times I_2 \dot{\omega}_0. \end{aligned} \quad (16)$$

The analysis presented in this section can be used to determine joint forces and moments for arbitrary motions of the ankle while the shank is inertially fixed. During walking shank is not inertially fixed and the rear foot experiences large ground reaction forces during heel strike. This device can be used for walking experiments by adding a second force torque sensor between the rear foot and ground and by recording the motion information of the shank. These modifications are subject of future work.

5 Experimental Results and Discussion

This section describes the experimental results obtained with the device. The experiments were performed with a healthy subject. Two sets of data were obtained when the user was asked to perform primarily: (i) motion about the D/P joint, (ii) motion about the P/S joint. The orientations of the D/P and P/S frames are shown in Fig. 5, this figure is representative of only the orientations of the frame and not the locations. The frames are placed at the actual joint in the human foot. The orientation information will be used in interpreting the results obtained.

In the first experiment, the subject was asked to perform dorsiflexion-plantarflexion without ground contact of the foot in the vertical position of shank. The ranges of rotation obtained are shown in Fig. 6. We can see that range of motion about the D/P axis is about $0.5rad$ and about P/S axis is about $0.15rad$. It can be seen that the frequency of motion is around $1Hz$, which is not very fast. Figs. 7 and 11 present the forces and torque applied by the subject about the D/P and P/S joints respectively. Due to the periodic rotational motion about the axes, the forces and torques are also oscillatory about a mean. M_z in Fig. 7 represents the torque about the D/P joint. Note that the peak dorsiflexor torque is around $16Nm$ and peak plantarflexor torque is around $2Nm$.

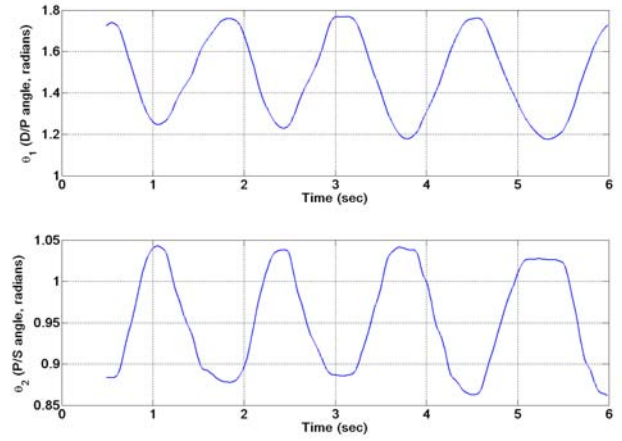


Fig. 6. The D/P (θ_1) and P/S (θ_2) angle movements during the motion about the D/P joint. There is some movement about the P/S axis but is small as compared to the D/P movement.

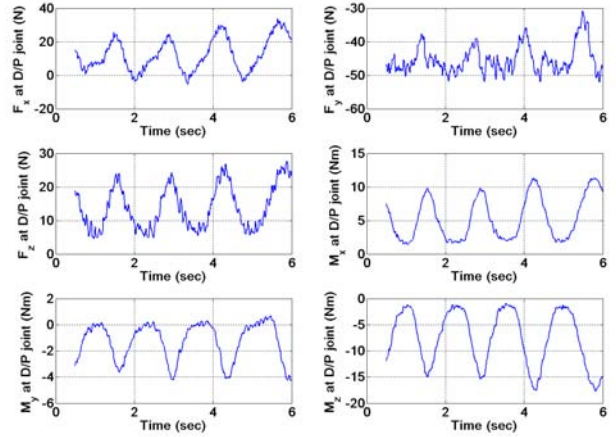


Fig. 7. The forces and moments applied by the subject about the D/P joint during the motion about the D/P joint.

According to the study by Weiss et. al. [14] the peak dorsiflexor torque range in his study is $3 - 14Nm$ with a mean of around $7Nm$ and the peak plantarflexor torque has range $0 - 5Nm$ with a mean of around $2Nm$. The values that we are seeing are in the higher side of this range due to the added weight of the device. In the next paragraph, we reason out the force and torque values observed based on the weight of the device and location of center of mass of various segments.

First, we examine the forces at the D/P joint in Fig. 7. The net torque applied by the shank to the foot at the D/P joint obtained by taking square root of the sum of squares of all the three components of moment, is about $8.5Nm$. The weight of foot is about $1Kg$ and the weight of the relevant parts of orthosis is about $3Kg$, and the center of mass of the this weight is $20cm$ from the D/P joint. This gives a torque of $8Nm$. Because there is some friction at the joints of the

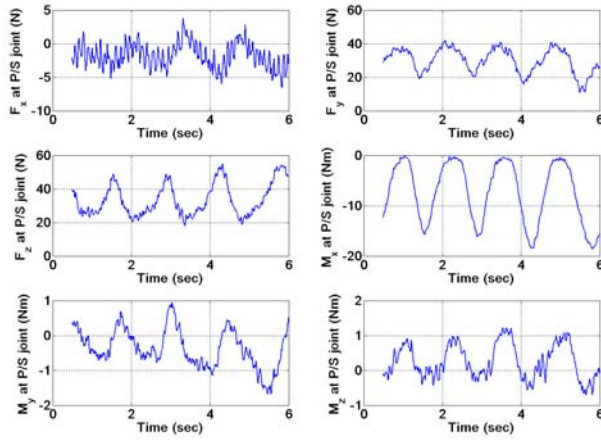


Fig. 8. The forces and moments applied by the subject about the P/S joint during the motion about the D/P joint.

device the subject has to apply torques to overcome that as well, this explains the slightly higher magnitude of the experimental mean torque. From Fig. 5, we see that the X and Z axes are almost in the horizontal plane, thus the torques about these axes are relatively large as compared to the Y-axis. The direction of the Z axis is such that the shank has to apply a negative torque to balance the torque due to the weight of device and foot, consistent with the experimental data. The net force applied by the shank to the foot at the D/P joint is about $46N$. Because the total foot and device weight on the D/P joint is also about $4Kg$, the calculated force is about $40N$, which is about $6N$ less than the mean of measured forces. This discrepancy can be attributed to friction. From Fig. 5, Y axis is pointing almost vertically downwards. Thus, the maximum force component of $43N$ is about this axis and is negative because the shank has to apply an upwards force at this joint to balance the gravitation force. The other two components, though small compared to the Y component, should not be expected to be zero because none of the axes are perfectly in a vertical or horizontal plane. Next, the forces applied by the subject at the P/S joint, in Fig. 11, are examined. An important point to note is that the mean moment of $0.3Nm$ about the P/S axis (M_z in Fig. 8) is very small as compared to the mean moment $7Nm$ about the D/P axis (M_z in Fig. 7). This is because during this experiment the subject was asked to perform a frontal plane dorsiflexion-plantarflexion movement, with no deliberate movement about the P/S joint. For the other two torque components, M_x has a sizeable magnitude of around $7Nm$. From Fig. 5, we see that the X axis is almost in the horizontal plane and nearly parallel to the D/P axis. Because the P/S joint is located near the D/P joint, this component of torque should be similar to the torque about the D/P axis which we observed. Also as shown in Fig. 5, the direction of the X axis is such that the terminal part gets negative torque from the previous segment to balance the gravitational torque. The net force component at the P/S joint is about $43N$. This is

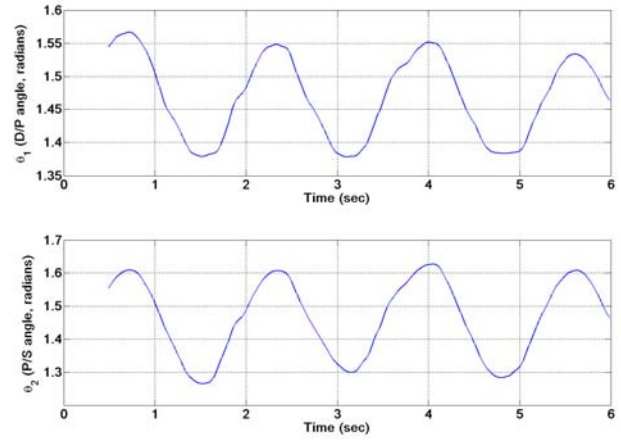


Fig. 9. The D/P (θ_1) and P/S (θ_2) angle movements during the motion about the P/S joint. It is difficult for a subject to obtain a pure P/S rotation but still we can see that P/S motion here is much more pronounced and the D/P motion is much less as compared to the previous case

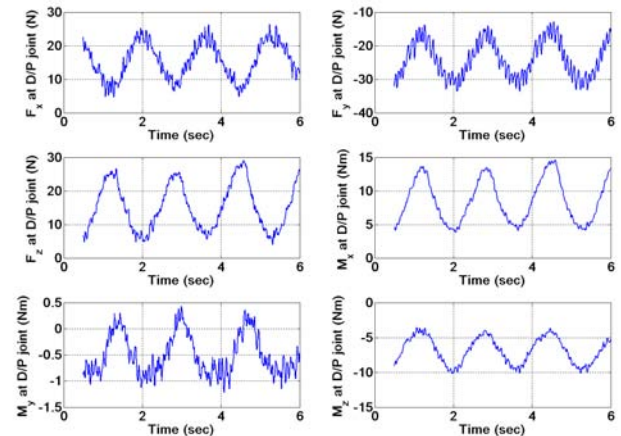


Fig. 10. The forces and moments applied by the subject about the D/P joint during the motion about the P/S joint.

due to the weight of the foot and the device. The terminal part of the orthosis and the foot are the heavier segments, so the force at the P/S joint is only slightly less than the force at the D/P joint. Fig. 5 also shows that the X axis is almost horizontal and hence has a small mean force of about $1N$ and that the X and Z axes are in the vertical plane both pointing in the upward direction and thus get major positive contributions due to the weight.

In the second experiment, the subject was asked to execute only the pronation-supination motion without ground contact of the foot. During this experiment the range of motion about the P/S axis is $0.35rad$ and about D/P axis is $0.2rad$, as shown in Fig. 9. We can see that the P/S motion here is much more pronounced and the D/P motion is

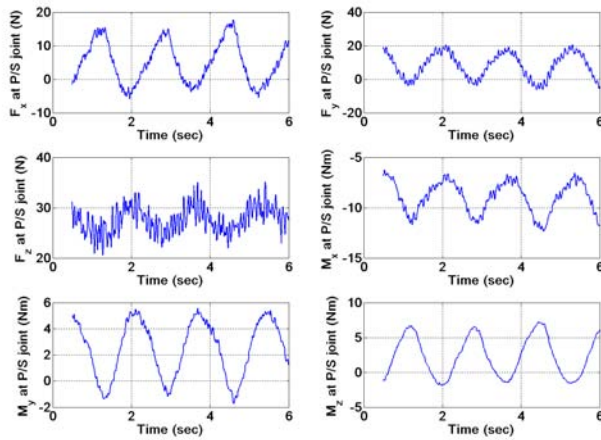


Fig. 11. The forces and moments applied by the subject about the P/S joint during the motion about the P/S joint.

much less as compared to the previous case. Fig. 10 shows the forces and torques exerted by the human at the D/P joint during P/S rotation. Comparing these results with the corresponding results for the previous experiment in Fig. 7, we see that, as expected, the means of forces and torques are still roughly the same but the amplitude of oscillation has reduced. For example, the amplitude of the torque about the D/P joint previously (M_z in Fig. 7) was $14Nm$ and is now $6Nm$ (M_z in Fig. 10). This is because the D/P rotation is considerably diminished as compared to the previous experiment. Fig. 11 gives the forces and torques at the P/S joint. Comparing this with the corresponding plot for the previous experiment (Fig. 8), we observe a sizeable increase in the torque about the P/S axis (M_z in both the figures), because the P/S motion is much more pronounced here.

6 Conclusions

In this paper, an innovative two degree-of-freedom ankle-foot orthosis is presented. The orthosis has two degrees-of-freedom that allow both dorsiflexion-plantarflexion and pronation-supination motion. Both axes are fitted with digital encoders. The device also has two force-torque sensors in its design. The device can be used as a stand alone measurement device to measure forces and torques. In this paper, the kinematic and design details of the orthosis are described. The Newton-Euler analysis of the device was used to convert the raw sensor data into the forces and torques generated by the subject with the foot. The experimental results for a healthy subject are presented and analyzed. In the future, this device will be redesigned to reduce its weight and an actuator will be added so that it can be used as a training device to restore a normal walking pattern.

Acknowledgements

The authors would like to thank Trisha Kesar, graduate student in the Interdisciplinary Graduate Program in Biome-

chanics and Movement Sciences, for valuable discussions during the course of this work. This research was supported by NIH grant # 1 R01 HD38582.

References

- [1] D. P. Ferris, J. M. Czerniecki, and B. Hannaford, "An ankle foot orthosis (AFO) powered by artificial muscles", *In Proc. 25th Annu. Meeting American Society of Biomechanics*, San Diego, CA, 1999.
- [2] S. Yamamoto, M. Ebina, S. Kubo, T. Hayashi, Y. Akita, and Y. Hayakawa, "Development of an Ankle-Foot Orthosis with Dorsiflexion Assist, Part 2: Structure and Evaluation", *Journal of Prosthetics and Orthotics*, Vol 11, Num 2, p 24, 1999.
- [3] J. A. Blaya and H. Herr, "Adaptive Control of a Variable-Impedance Ankle-Foot Orthosis to Assist Drop-Foot Gait", *IEEE Tran. on Neural Systems and Rehab. Engg.*, Vol. 12, No. 1, March 2004.
- [4] S. K. Abu-Hasaballah, M. D. Nowak, P. D. Cooper, "Enhanced Solid Ankle-Foot Orthosis Design: Real-time contact pressures evaluation and finite element analysis", *American Society of Mechanical Engineers, Bioengineering Division (Publication) BED*, v 36, *Advances in Bioengineering*, 1997, p 285-286.
- [5] K. Italiano, C. Macedo, S. Veranis, K. Callahan, "Techniqyges of Weight Reduction of Polypropylene Ankle-Foot Orthosis", *Association for the Advancement of Rehabilitation Technology*, 1986, p 126-128 .
- [6] S. K. Agrawal, A. G. Erdman, Biomedical Assist Devices and New Biomimetic Machines A Short Perspective, *Journal of Mechanical Design*, v 127, 2005, p. 799-801.
- [7] M. Nordin, V. H. Frankel, "Basic Biomechanics of the Musculoskeletal System", Lippincott Williams & Wilkins; 3 edition, 2001.
- [8] Inman, V.T., "The joints of the ankle", Baltimore Williams & Wilkins; 1976.
- [9] A. Leardini, J.J. OConnor", F. Catani, and S. Giannini, "Kinematics of the human ankle complex in passive flexion: a single degree of freedom system", *Journal of Biomechanics*, v 32, n 2, 1999, p. 111-8.
- [10] A. Lundberg, "Kinematics of the ankle and foot. In vivo roentgen stereophotogrammetry", *Acta Orthopaedica Scandinavica Supplementum*, v 233, 1989, p. 1-24.
- [11] D.G. Wright, S.M. Desai, and W.H. Henderson, "Action of the subtalar and ankle-joint complex during

the stance phase of walking”, *Journal of Bone and Joint Surgery*, v 46-A, 1964, p. 361-382.

- [12] M. Bottlang, J.L. Marsh, and T.D. Brown, ”Articulated external fixation of the ankle: minimizing motion resistance by accurate axis alignment”, *Journal of Biomechanics*, v 32, n 1, 1999, p. 63-70.
- [13] NASA Reference Publication 1024, “Anthropometric Source Book: Volume I: Anthropometry for Designers”, NASA, 1978.
- [14] P.L. Weiss, R.E. Kearney, I.W. Hunter, ”Position Dependence of Ankle Joint Dynamics-I”, *Journal of Biomechanics*, v 19, n 9, 1986 pp. 737-51.